# Application of a diffraction-corrected ray theory to the slot lens in acoustic microscopy

Dmitry Chizhik and Douglas A. Davids
*Department of Electrical Engineering, Polytechnic University, Brooklyn, New York 11201*

(Received 8 May 1992; accepted for publication 13 August 1992)

A modified ray approach is used to model the slot lens for determining $V(z)$ and the results are compared with experiment for several materials. The slot lens is also used to obtain $V(z)$ of $y$-cut quartz for a number of slot orientations relative to the crystalline $x$ axis. The Rayleigh wave velocity as a function of propagation direction is then deduced from these measurements and compared with accepted values. It is shown that although the angular restriction of the slot lens is introduced in the lens aperture plane in contrast to shaped electrodes in the transducer plane, it is still necessary to account for diffraction in the lens rod in order to provide agreement with experiment. The application of the slot lens to crack detection is also examined and an analysis provided that yields substantial agreement with experiment. A simple yet effective method for extracting the surface wave reflection coefficient of a crack from measurements is proposed and demonstrated.

PACS numbers: 43.20.Dk, 43.85.Ls

## INTRODUCTION

The slot lens used in scanning acoustic microscopy is illustrated in Fig. 1. It employs a circular transducer together with a lens aperture that is restricted by an acoustic absorber to provide surface wave excitation on the object surface over a restricted range of azimuth angles. Such systems have been shown not only to have application in the study of homogeneous anisotropic materials, as for example, in determining the angular dependence of Rayleigh velocity, but when employed in the raster-scanning mode, they permit the formation of images in a manner similar to the point-focus lens. Such capabilities have been demonstrated in the case of structured surfaces[1] and polycrystalline samples. The slot lens evolved from an earlier lens having a bow-tie-shaped electrode[2] that, owing to diffraction in the lens rod, gave rise to a significantly greater than expected angular spectrum of surface waves which resulted in an inability to measure accurately the Rayleigh-wave velocity along specific directions.[3] To avoid the slit-like character of the bow-tie acoustic radiator and attendant radiation pattern, the slot lens uses a circular transducer to produce an axially symmetric acoustic field at the rear aperture of the lens. The concave focusing surface is partially filled with an acoustic absorbing material to form a slot-shaped clear area that limits the angular spread of acoustic rays in azimuth. Later work to be described here, shows that the slot lens may also be used to advantage in crack detection applications as the restriction in the direction of the surface waves that are excited permits an estimation of the reflection and transmission coefficients of the crack which may be related to the structure of the crack.

Unlike the line focus lens, the slot lens forms a point focus limited only by diffraction which permits superior resolution in imaging applications. In crack detection applications, the transducer voltage is monitored as a function of distance from the crack $x$. The analysis of the resultant response is simplified by assuming a straight crack of infinite length that corresponds in practice to requiring the crack to be larger than the interrogating acoustic beam. For the slot lens used here, straight cracks as small as 1 mm in length or longer slowly curving cracks satisfy this requirement for reasonable defocus distances. In addition, since the slot lens

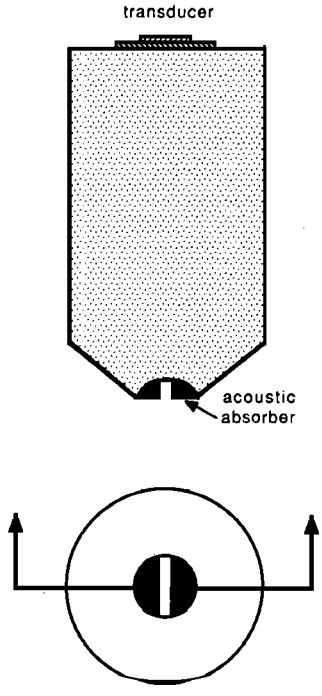


FIG. 1. Longitudinal cross section view of the slot lens. The transducer and lens rod have axial symmetry while the acoustic absorber blocks all but a slot-shaped area of the spherical lens surface.

 0001-4966/92/123291-11$00.80  

launches surface waves over a restricted angular spectrum, the crack need not be precisely perpendicular to the slot axis for crack detection, in contrast to the line focus lens.

As a number of useful applications have been documented for the slot lens, it would appear desirable to develop a theory to predict the behavior of the slot lens in order to better understand its operation and possibly to optimize its configuration. The application of a strictly geometric ray theory[4] to the slot lens geometry for the purpose of predicting the acoustic material signature or $V(z)$ yields poor agreement with measurement. This suggests that the effects of diffraction, especially in the relatively long path length of the lens rod, should be taken into account in order to provide better agreement. A similar problem was found in the case of the point-focus lens, and was treated by diffraction corrections to the geometric ray theory.[5] In this work, the diffraction corrected ray theory is adapted to the lower symmetry slot lens in order to improve the prediction of transducer response for isotropic samples that are defect free or those that contain a long surface breaking crack.

Somekh *et al.*[6] derived an approximate Green's function for the line focus acoustic microscope and used it to numerically evaluate $V(x)$ in the presence of a surface breaking crack. Rebinsky and Harris[7] have applied asymptotic approximations to evaluate the integral expressions for the response of the line focus microscope both for cracked and defect free samples. They have also proposed a method to evaluate the crack surface acoustic wave (SAW) reflection coefficient from the acoustic signature of the crack. Beside the achievable but nontrivial requirement that the microscope be capable of measuring both amplitude and phase, the proposed method requires such additional information as SAW attenuation, amplitude of the illumination over the lens aperture, and the exact position of the lens relative to the crack.

In this work, a robust method to extract the surface acoustic wave reflection coefficient from a line scan measurement $V(x)$ using the slot lens is proposed and demonstrated. The method requires only knowledge of the SAW velocity, which is easily deduced from a $V(z)$ measurement made in a defect free region of the sample.

## I. THEORETICAL MODELING OF $V(z)$ FOR THE SLOT LENS ACOUSTIC MICROSCOPE

### A. Calculation of the specularly reflected contribution $V_G(z)$

A diffraction-corrected ray approach has been successfully applied to predict the complex phasor $V(z)$ response of a point focus acoustic lens having a circular aperture.[5] In that work, the effective transducer field illuminating the lens aperture is solved numerically using the theory of Tjotta and Tjotta for the field of a piston radiator[8] and the result is approximated by a sum of Gaussian functions of the form $\Sigma_i A_i \exp(-\rho^2/B_i^2)$ in order to permit an analytic evaluation of the resulting integral. For the lens used in this work, $A_1 = 1.35, B_1 = 1000\mu\text{m}, A_2 = 0.58$, and $B_2 = 2700\mu\text{m}$. A more general expression for $V_G(z)$ for a lens that does not necessarily have an axially symmetric aperture may be written as

$$V_G(z) = -\frac{T_{LW}(0)T_{WL}(0)\mathscr{R}(0)\exp[2ik_w(D/n+f+z)]}{M} \times\frac{4}{\pi R_a^2}\int_0^{\pi/2}\int_0^{R_a}\exp\left(\frac{ik_w\rho^2}{2n(-u)}\right) \times\sum_i \mathscr{A}_i\exp\left(\frac{-\rho^2}{\mathscr{B}_i^2}\right)P\left(\frac{\rho}{M},\phi\right)P(\rho,\phi)\rho\,d\rho\,d\phi, \quad (1)$$

with

$$\mathscr{A}_l = A_iA_j, \quad \frac{1}{\mathscr{B}_l^2} = \frac{1}{B_i^2}+\frac{1}{(B_jM)^2},$$
$$i = 1,2, j = 1,2, \text{ and } l = 1,2,3,4,$$

and where, as in the referenced article, $T_{LW}(0)$ and $T_{WL}(0)$ are the lens–water and water–lens transmission coefficients at the angle $\theta = 0$, which corresponds to the normally incident rays, $\mathscr{R}(0)$ is the water-sample reflection coefficient at normal incidence, $D$ is the transducer–lens aperture separation, $R_a$ is the aperture radius, $f$ is the focal length of the lens in water, and $n$ is the acoustic index of refraction of the lens material relative to water. Additionally, $M = |f+2z|/f$ and $u = f(f+2z)/2nz$. The pupil function of a lens having a slot aperture of half-width $w$ can be expressed in terms of the cylindrical coordinates $\rho$ and $\phi$ as

$$P(\rho,\phi) = \text{circ}\left(\frac{\rho\cos\phi}{w}\right)\text{circ}\left(\frac{\rho}{R_a}\right),$$

where

$$\text{circ}(x) = \begin{cases}1, & 0\leqslant x\leqslant 1,\\ 0, & x>1.\end{cases}$$

In (1) the integration over $\phi$ need be carried out only from 0 to $\pi/2$, owing to the fourfold symmetry of the slot aperture. A factor of 4 is then introduced in order to account for the contribution of all four quadrants. The integration over $\rho$ can be carried out analytically, resulting in the expression

$$V_G(z) = -\frac{T_{LW}(0)T_{WL}(0)\mathscr{R}(0)\exp[2ik_w(D/n+f+z)]}{\pi R_a^2 M} \times 4\int_0^{\pi/2}\sum_i \mathscr{A}_i\frac{n\mathscr{B}_i^2(-u)}{ik_w\mathscr{B}_i^2-2n(-u)} \times\left[\exp\left(\frac{ik_w\rho_T^2}{2n(-u)}\right)\exp\left(\frac{-\rho_T^2}{\mathscr{B}_i^2}\right)-1\right]d\phi, \quad (2)$$

where

$$\rho_T = \begin{cases}w_1/\cos\phi, & \phi<\cos^{-1}(w_1/R_a),\\ R_a, & \phi>\cos^{-1}(w_1/R_a),\end{cases}$$

and

$$w_1 = \begin{cases}wM, & z<0,\\ w, & z>0.\end{cases}$$

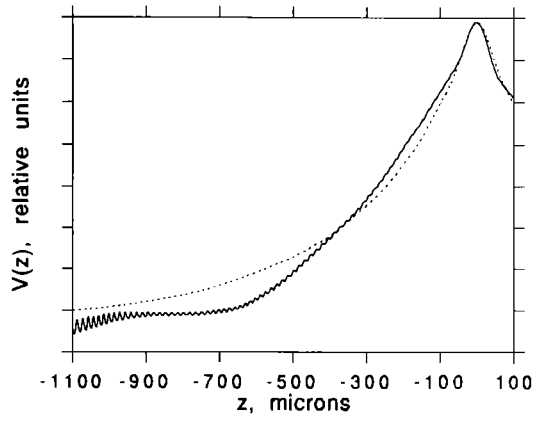


FIG. 2. Plot of $V(z)$ of Teflon for a slot aperture lens: observed (solid) and calculated using the diffraction-corrected ray approach (dashed).

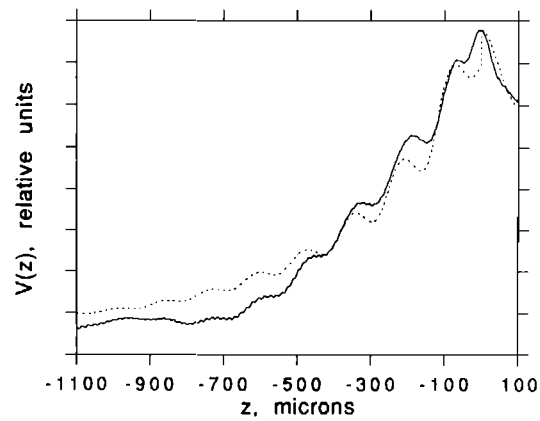


FIG. 3. Plot of $V(z)$ of glass for a slot aperture lens: observed (solid) and calculated using the diffraction-corrected ray approach (dashed).

As the existence of the slot aperture destroys the axial symmetry of the lens, the above integral can no longer be evaluated analytically, consequently numerical integration is employed. The result of this calculation is plotted in Fig. 2 and compared with a measured $V(z)$ for a sample made from Teflon, taking advantage of the fact that the water–Teflon interface does not support leaky surface modes. The agreement with the observed data is not as good as it is in the case of a circular aperture lens,[5] which could be due, at least in part, to the fact that the strict geometric approach ignores diffraction in water, which, owing to the truncating effect of the slot, may be more important in the present case.

An advantage of the ray approach outlined above is that, in addition to a gain in physical insight, it requires only a single integration over $\phi$ while the angular spectrum method requires the evaluation of a much more computationally intensive double integral over the coordinates $x$ and $y$.

### B. Calculation of the leaky contribution $V_L(z)$

In the strict geometric ray method of analysis of the point-focus lens of Bertoni,[4] leaky rays that emanate from the sample surface form a ring focus of radius $\rho_R$ in the cylindrical lens rod. The slot aperture causes portions of this ring to be truncated. Thus, neglecting the effects of diffraction, the leaky contribution $V_L(z)$ in the slot lens is the same as for a circular lens but scaled by the ratio of the length of arc exposed by the slot to the total circumference of the focal ring or, approximately,

$$V_L(z) = V_{L\,\mathrm{circ}}(z)\,\frac{2\sin^{-1}(w/\rho_R)}{\pi}, \tag{3}$$

where $w$ is the half-width of the slot.

### C. The total voltage $V(z)$

The total voltage response $V(z)$ of the slot aperture lens for a sample that supports leaky surface waves is obtained by adding the complex quantities $V_G(z)$ and $V_L(z)$. The magnitude of $V(z)$ is plotted in Fig. 3 for comparison with laboratory measurement of a lens having a slot of 1.5-mm aperture width. It should be noted that the observed $V(z)$ falls off more rapidly than the theoretical prediction which may involve the neglect of diffraction in the couplant here as well. This effect was also evident in the $V_G(z)$ of Fig. 2.

## II. THE DETERMINATION OF THE RAYLEIGH WAVE VELOCITY $v_R(\phi)$ OF AN ANISOTROPIC MATERIAL BY MEANS OF THE SLOT LENS

A 50-MHz point-focus lens that was modified to have a slot width of 1 mm was used to make $V(z)$ measurements of a $y$-cut quartz sample over a range of slot orientations relative to the crystalline $x$ axis. For illustration, a $V(z)$ curve measured at an azimuthal angle between the slot and crystal $x$ axis $\phi = 90°$ is shown in Fig. 4. To obtain the Rayleigh wave velocity $v_R$ as a function of the surface-wave propagation direction $\phi$, the $V(z)$ curves were processed using an algorithm proposed by Briggs.[9] The resulting values of $v_R(\phi)$ are plotted in Fig. 5 along with the accepted dispersion curve $v_R(\phi)$ cited by Kushibiki *et al.*[10] Since $y$-cut quartz has fourfold symmetry, only the range $0 < \phi < 90°$ need be displayed. The largest error in $v_R$ is observed to be about 1%. This demonstrates that the slot lens does indeed launch Rayleigh waves in a reasonably narrow range of di-

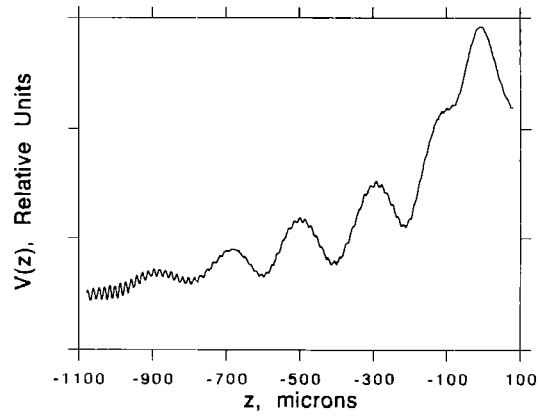


FIG. 4. Observed $V(z)$ of $y$-cut quartz with slot oriented at 90° to the crystalline $x$ axis.

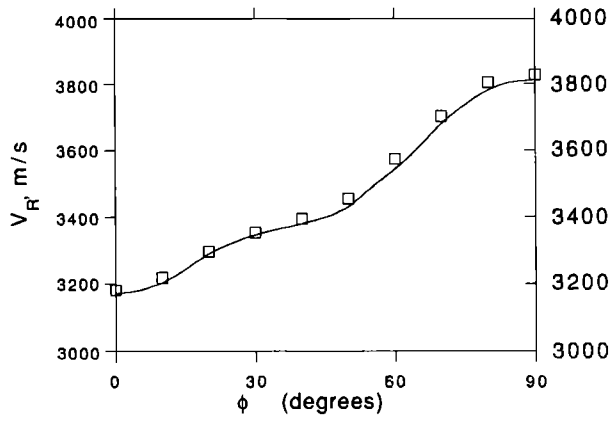


FIG. 5. Rayleigh wave velocity $v_R$ of $y$-cut quartz as a function of direction of propagation angle $\phi$ measured from the crystalline $x$ axis: accepted (solid line) and measured values using the slot lens (open boxes).

rections and therefore can be used to measure Rayleigh wave velocities as a function of propagation direction in an anisotropic crystal.

## III. MODELING OF $V(x)$ MEASUREMENTS ACROSS A SURFACE BREAKING CRACK USING THE MODIFIED RAY THEORY

In a previous article involving the current authors,[11] a modified ray theory for the point focus lens was used to predict the microscope response of a sample surface containing a surface-breaking crack. The defect is assumed in the reference to be of infinitesimal thickness, straight, symmetrical in a planar surface and long compared with the diameter of the spot produced by the incident acoustic beam, even at maximum defocus. Of particular interest are line-scan measurements, called $V(x,z_0)$, obtained by maintaining the lens at a constant defocus distance $z_0$ and scanning in $x$ perpendicular to the discontinuity. The displacement variable $x$ is defined as the distance between the lens axis and the crack, with $x = 0$ corresponding to the lens being centered directly above the crack. The crack is assumed to lie parallel to the $y$ direction. In this work, the analysis presented in the referenced article will be extended to the slot aperture lens.

The total voltage response $V(x,z)$ of the microscope for a planar sample, whose surface contains a crack that meets the above requirements, may be expressed as

$$V(x,z) = V_G(z) + V_T(x,z) + V_{\text{refl}}(x,z), \qquad (4)$$

where $V_G(z)$ is the specularly reflected component, $V_T(x,z)$ is due to the leaky waves transmitted through the crack as well as those leaky waves that propagate unimpeded past the crack, and $V_{\text{refl}}(x,z)$ is the contribution of the leaky waves scattered from the crack. The ray paths involved in determining these contributions in the vicinity of the crack are shown in Fig. 6. Here both the crack and the lens are assumed to have inversion symmetry, $V(x,z) = V(-x,z)$, i.e., the same response is detected on either side of the crack. It will be assumed that when a surface wave strikes a crack, a portion of the incident wave is transmitted with a field trans-

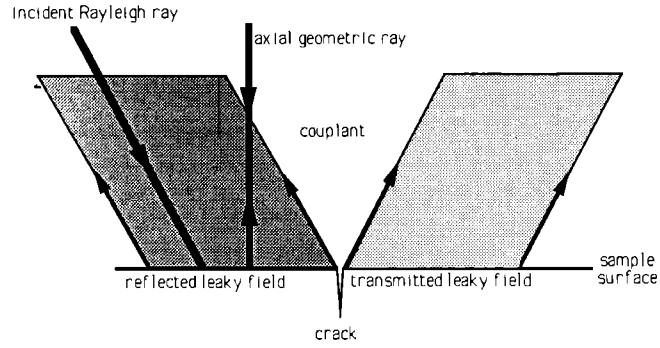


FIG. 6. Ray paths for the transducer voltage components $V_G$, $V_T$, and $V_{\text{refl}}$. The component $V_G$ results from the axial ray, $V_{\text{refl}}$ from the reflected leaky field, and $V_T$ from the transmitted leaky field.

mission coefficient $T$, and a portion is reflected with a field reflection coefficient $R$. The dependence of $T$ and $R$ on the angle of incidence of the surface wave will be ignored on the basis that the predicted variation near normal incidence is weakly dependent on angle, as shown by Angel and Achenbach,[12] moreover, for the slot lens, the range of incident angles is limited to near normal incidence.

As the crack is assumed to be of infinitesimal thickness, the specularly reflected component $V_G(z)$ is unperturbed by the crack and hence must be independent of $x$. Thus, $V_G(z)$ is evaluated using expression (2).

### A. Transmitted component $V_T(x,z)$

Figure 7 illustrates the leaky ray structure for a defect-free sample when the lens is closer than the focal distance or

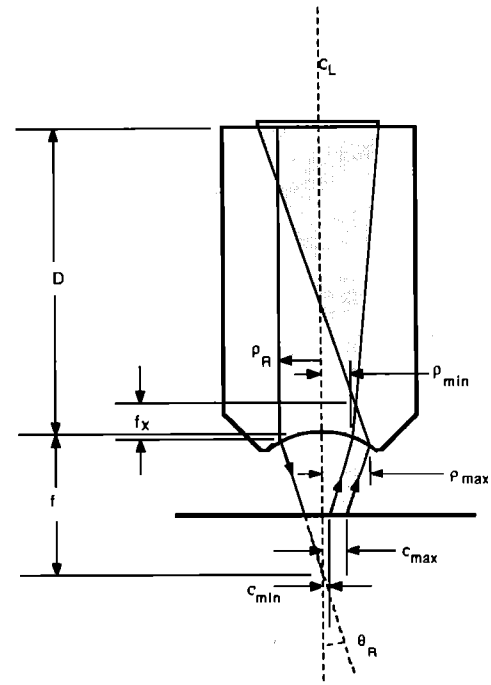


FIG. 7. Leaky ray bundle in the $x$–$z$ plane. The shaded region delineates those rays that ultimately excite the transducer. For clarity of the figure, only the ray perpendicular to the transducer is shown as exciting the surface wave.

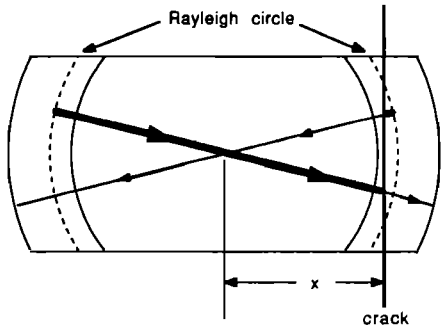


FIG. 8. Geometry of a surface ray that is excited on the left and leaks energy to the right of lens axis. After the ray crosses the crack the leaky field is reduced by the factor $T$. A left propagating ray is also shown.

$z<0$. This illustration applies to any radial plane that is not restricted by the slot aperture. For clarity, only surface waves launched on the left and detected on the right are shown. Note that the leaky contribution to the transducer voltage is due to a ray bundle that originates from a region on the sample surface that has the shape of two sections of a ring, shown in Fig. 8, bounded by circles of radii $c_{\min}$ and $c_{\max}$ and the projection of the slot aperture onto the sample surface; see also Figs. 7 and 9. In the following, this ring is referred to as the Rayleigh ring.

When the crack is sufficiently displaced from the lens axis, some surface rays are leaked into the couplant without having been scattered by the crack, and therefore contribute to the transducer voltage as in the defect-free case. However, the component of voltage due to those rays that are transmitted through the crack is scaled by the crack transmission coefficient $T$, as is shown also in Fig. 8 by the thickness of the ray bundle.

Transmitted contribution $V_T(x,z)$ is given by

$$V_T(x,z) = V_L(z)\,[Q_R(x,z) + Q_L(x,z)], \tag{5}$$

where $V_L(z)$ is the contribution to the $V(z)$ due to the leaky surface waves for the defect-free surface, and $Q_R(x,z)$ and $Q_L(x,z)$ are fractional contributions to $V(x,z)$ from the rays re-radiated into water on the right and left sides of the lens, respectively, as shown in Fig. 8. In the absence of a crack $Q_R = Q_L = 0.5$.

The $V_T(x,z)$ contribution to the $V(x,z)$ is assumed to be proportional to the total field flux leaked into water represented by the area shown as shaded in Fig. 7. This assumption is most valid for a relatively long lens rod where the

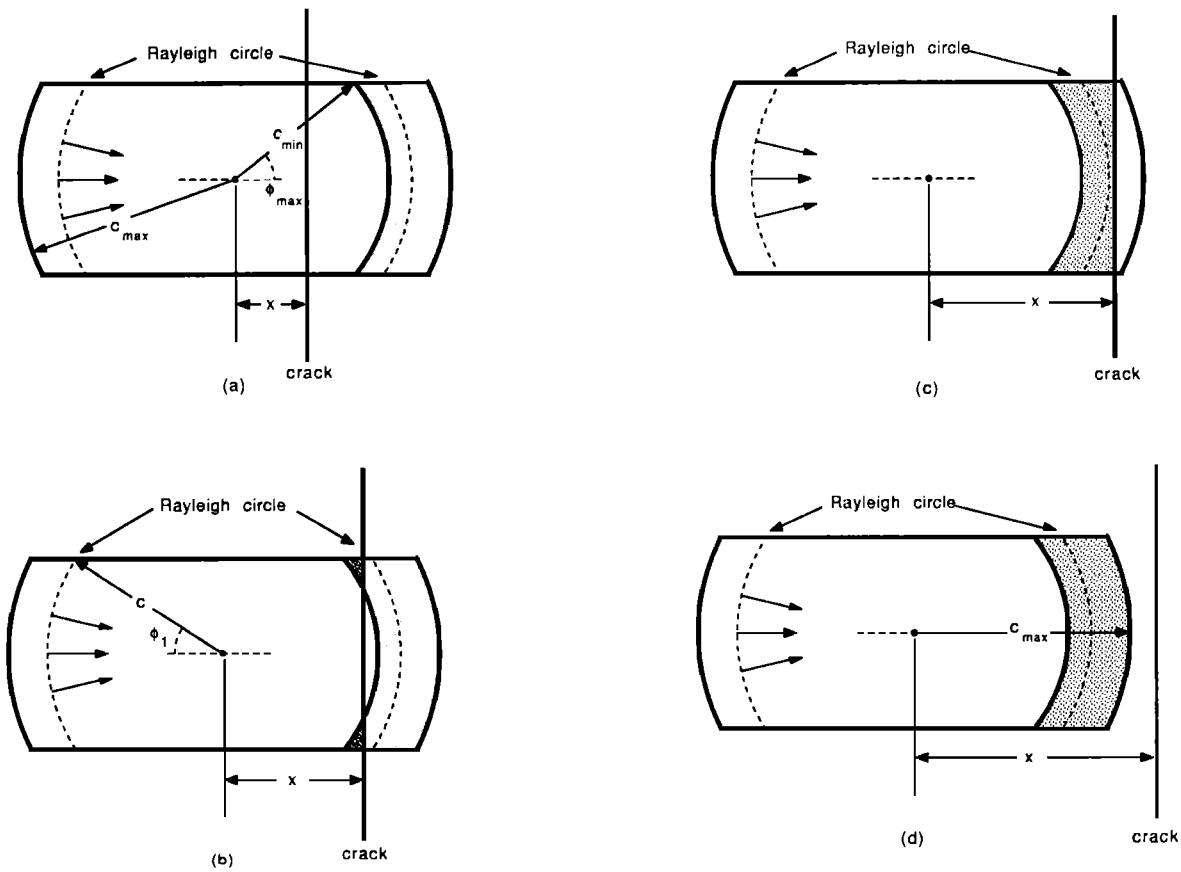


FIG. 9. Distinct ranges of crack displacement that lead to different geometric relations in determining $Q_R$: (a) $0<x<c_{\min}\cos\phi_{\max}$, (b) $c_{\min}\cos\phi_{\max}<x<c_{\min}$, (c) $c_{\min}<x<c_{\max}$, (d) $x>c_{\max}$. The region of leaky radiation that reaches the transducer is shown as shaded, with the more dense shading indicating leaky radiation resulting from surface waves that are unscattered by the crack.

phase variation of the field at the transducer is not as significant. The factor $Q_R$ can be seen to be

$$Q_R = \frac{QT + 1 - Q}{2}, \tag{6}$$

where $Q$ is the fraction of the ray flux intercepted by the crack and therefore scaled by the crack transmission coefficient $T$, and $(1 - Q)$ is the fraction of the ray flux that is unscattered. Under these conditions, the factor $Q$ can be expressed as:

$$Q = \frac{\text{Area of obstructed part of Rayleigh ring}}{\text{Total area of Rayleigh ring section}}. \tag{7}$$

The above relation makes use of the assumption that all leaky radiation source points contribute equally to $V_T(x,z)$. This approximation is based on the fact that as the area of the Rayleigh ring is relatively small and the amplitude of the radiated field varies slowly, it is reasonable to treat the field as though it has a constant amplitude over the ring section. The total area of the Rayleigh ring section may be found approximately from the relation $\phi_1 (c_{\max}^2 - c_{\min}^2)$, where $\phi_1$, illustrated in Fig. 9, is the effective half-angle of the ring arc, defined in terms of the slot half-width $w$ at the lens aperture by the relation

$$\phi_1 = \begin{cases} \sin^{-1}(w/\rho_R), & w < \rho_R, \\ \pi/2, & w > \rho_R. \end{cases} \tag{8}$$

All azimuthal angles $\phi$ are defined relative to the direction of the $x$ axis. As the lens is translated to the left along the $x$ axis, there are four distinct ranges of crack position $x$, shown in Fig. 9. In Fig. 9(a), $\phi_{\max}$ is the azimuthal angle coordinate that forms one of the boundaries of the Rayleigh ring arc, whose value defined at the lens aperture is

$$\phi_{\max} = \begin{cases} \sin^{-1}(w/\rho_{\min}), & w < \rho_{\min}, \\ \pi/2, & w > \rho_{\min}. \end{cases} \tag{9}$$

Using definition (9) and Fig. 9, $Q$ is found to be approximately given by

$$Q = \begin{cases} 1, & 0 < x < c_{\min} \cos\phi_{\max} \\ \dfrac{2}{\phi_1 (c_{\max}^2 - c_{\min}^2)} \displaystyle\int_{c_{\min}}^{c_{\max}} \rho \, d\rho \int_0^{\cos^{-1}(x/\rho)} d\phi, & c_{\min} \cos\phi_{\max} < x < c_{\min} \\ \dfrac{2}{\phi_1 (c_{\max}^2 - c_{\min}^2)} \displaystyle\int_x^{c_{\max}} \rho \cos^{-1}\left(\frac{x}{\rho}\right) d\rho, & c_{\min} < x < c_{\max} \\ 0, & x > c_{\max}. \end{cases}$$

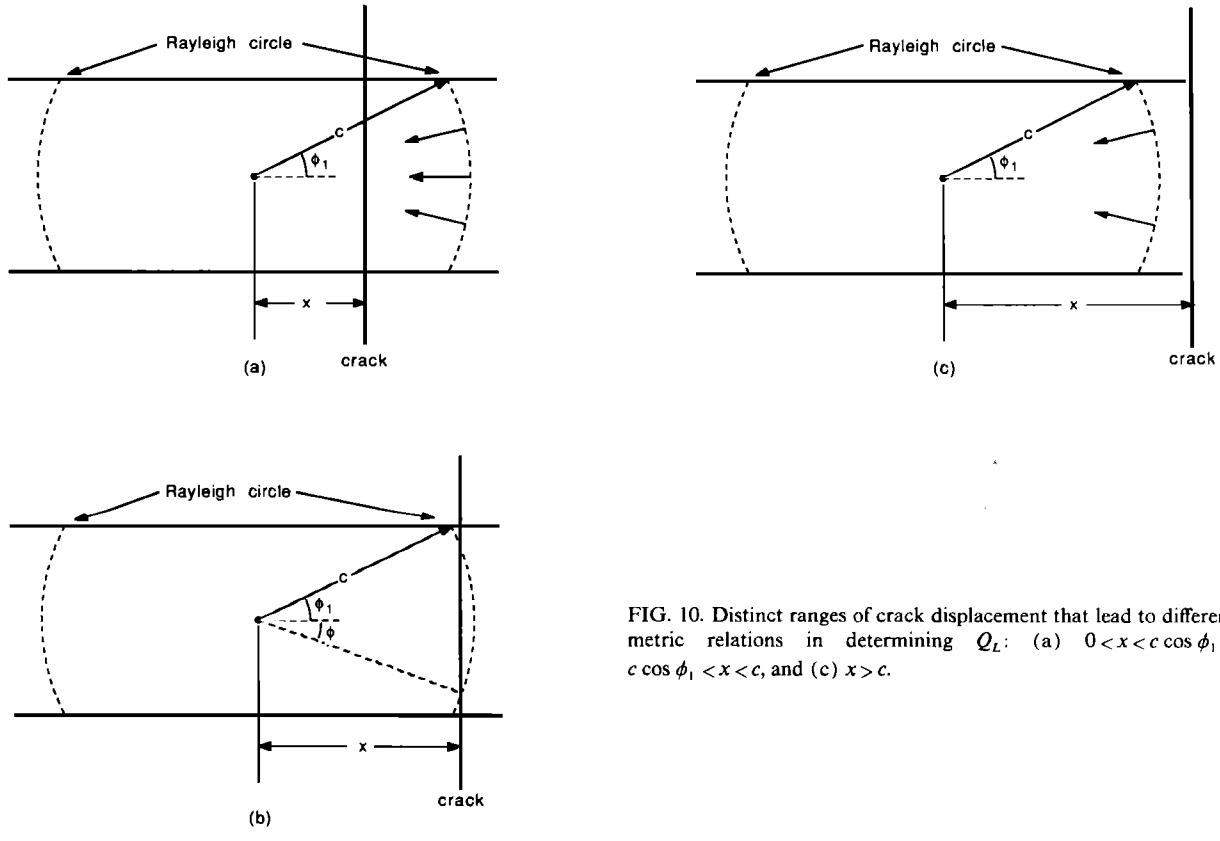


FIG. 10. Distinct ranges of crack displacement that lead to different geometric relations in determining $Q_L$: (a) $0 < x < c \cos\phi_1$, (b) $c \cos\phi_1 < x < c$, and (c) $x > c$.

For rays that are excited on the right and collected by the transducer on the left side of the crack there are three distinct regions of crack displacement $x$, shown in Fig. 10. The factor $Q_L$ is then found to be

$$Q_L = \begin{cases} T/2, & x < c\cos\phi_1, \\ 0.5\,\dfrac{2\phi T + 2(\phi_1 - \phi)}{2\phi_1} = \dfrac{\phi T + \phi_1 - \phi}{2\phi_1}, & c\cos\phi_1 < x < c, \\ 0.5, & x > c. \end{cases} \tag{11}$$

Here the angle $\phi = \cos^{-1} x/c$ and the radius of the Rayleigh circle $c = |z| \tan\theta_R$. The Rayleigh circle, as shown in Fig. 10, is a circle formed in the plane of the sample surface by rays incident at the angle $\theta_R$ from the normal.

The transmitted component $V_T(x,z)$ can be viewed as a reduction of the leaky component $V_L(z)$ due to the presence of the crack. The above analysis enables the determination of $V_T(x,z)$ for $z<0$. When $z>0$, the surface waves diverge away from the lens and, thus, there is no leaky component $V_L(z)$ intercepted by the transducer. Consequently, $V_T(x,z) = 0$ for $z>0$.

### B. Reflected surface wave contribution $V_{\text{refl}}(x,z)$ for $z<0$ and $x>c$

In Fig. 11, the reflected contribution to $V(x,z)$ has two components, defined by

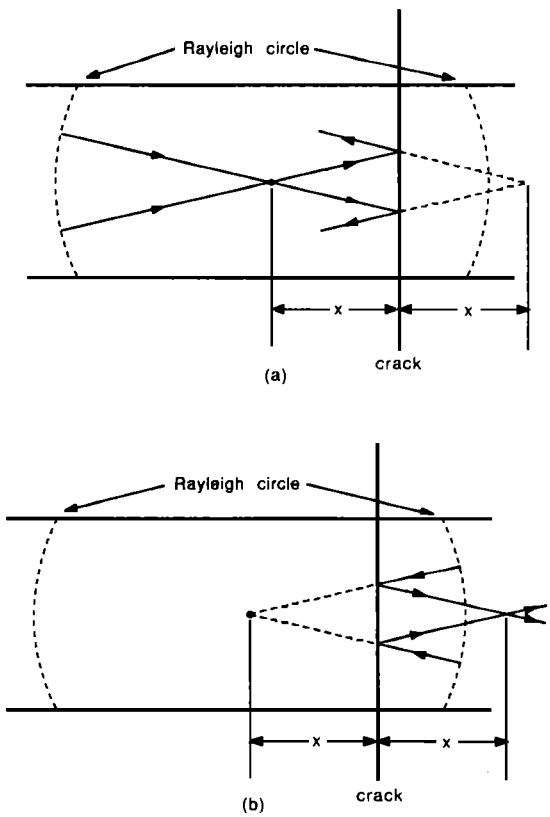


FIG. 11. Focusing of surface rays reflected from the crack on the (a) left and (b) right side of the Rayleigh circle.

$$V_{\text{refl}}(x,z) = V_{RR}(x,z) + V_{RL}(x,z), \tag{12}$$

where $V_{RR}$ is the contribution due to the surface waves incident on the discontinuity from the right [Fig. 11(b)] and $V_{RL}$ is due to the waves incident from the left [Fig. 11(a)]. Further examination of the figure reveals that $V_{RR} = 0$ for $x>c$ and $z<0$. In this case the only contribution to $V_{\text{refl}}$ is from the left. Let $V_{\text{refl}}(x,z) = V_R(x)$ in this range.

The expression for the field illuminating the transducer was found in Ref. 11 in the case of a point-focus lens, and is generalized here to include the effects of a slot aperture.

Integrating the field over the transducer and normalizing to the transducer area,

$$V_R(x) = RT_{LW}(\rho_R)T_{WL}(\rho_R)E \times \exp 2ik_w(D/n + f + z\sec\theta_R) \times \exp 2ik_p(x - z\tan\theta_R)\exp\left(-\frac{i3\pi}{2}\right)\sqrt{\frac{ff_x}{n}} \times \frac{\rho_R}{D\sqrt{2|x|c}}K_1(x), \tag{13}$$

where, from Ref. 4,

$$E = -2\alpha_L\sqrt{\frac{2\pi|z|}{k_w\cos^3\theta_R}}\exp\left(-\frac{i\pi}{4}\right),$$

the Rayleigh pole $k_p = k_R + i\alpha_R$, and

$$K_1(x) = \frac{1}{\pi R_T^2}\int_{\text{transducer}}\sqrt{\frac{D}{D-f_y}}P_1(y_1) \times \exp\frac{ik_w(x_1-\rho_R)^2}{2nD}\exp\frac{ik_w y_1^2}{2n(D-f_y)}\,dx_1\,dy_1. \tag{14}$$

In (14) the pupil function $P_1(y_1)$ accounts for the spatial restriction of the beam by the lens aperture. Projecting the slot aperture onto the plane of the transducer as illustrated in Fig. 12, the pupil function is found to be $P_1(y_1) = \text{circ}(y_1/y_{\max})$, where $y_{\max} = w|D-f_y|/|f_y|$. The locations of the astigmatic foci $f_x$ and $f_y$ were found in Ref. 11 to be

$$f_x = f - R_0 \tag{14a}$$

and

$$f_y = \frac{(f-R_0)\rho_R}{2x} + f_x, \tag{14b}$$

where $R_0$ is the lens radius of curvature.

### C. The reflected contribution $V_{\text{refl}}(x,z)$ for $z<0$ and $x<c$

The entire reflected voltage contribution $V_{\text{refl}}(x,z)$ will now be considered when the crack lies within the Rayleigh circle, i.e., $z<0$ and $x<c$, shown in Fig. 11(a). The rays incident from the left give exactly the same expression as found for $V_R(x)$ except that for $f_y > D$ there is only one astigmatic focus in the lens rod, which corresponds to $0 < x < (f-R_0)\rho_R/2(D-f_x)$. In this case the ray field does not suffer a $-\pi/2$ phase shift due to passing through the focus in the corresponding range of $x$, or explicitly

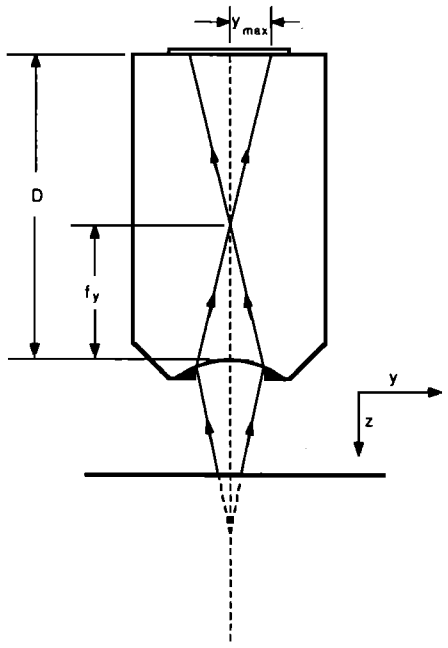


FIG. 12. Illumination of the transducer by a bundle of leaky rays that are reflected from the crack, shown in the $y$–$z$ plane.

$$V_{RL}(x) = \begin{cases} V_R(x)\exp(i\pi/2), & \\ & 0 < x < 2(D - f_x)/[(f - R_0)\rho_R], \\ V_R(x), & \text{otherwise.} \end{cases} \tag{15}$$

To find the contribution due to rays incident on the right, $-x$ should replace $x$ in expression (13). As shown in Fig. 11(b), the Rayleigh waves are reflected from the crack before reaching the focus at the lens axis. The reflected rays will still converge to a focus located a distance $2|x|$ from the lens axis. If $2|x| > c$, the rays will leak into water and focus above the sample surface. In either case, a real focus is formed and the previous expression derived for $V_R(x,z)$ applies. It should also be noted that since $f_y < 0$ for $|x|$ small and $x < 0$, there is only one real focus in the lens rod and therefore

$$V_{RR}(x,z) = V_R(-x,z)\exp(i\pi/2). \tag{16}$$

As $|x|$ increases, $f_y$ for $V_{RR}(x,z)$ determination will eventually become positive, however, in this case the crack will be outside the Rayleigh circle for practical defocus distances $z$ and hence $V_{RR}(x,z) = 0$ for $|x| > c$.

### D. The reflected contribution $V_{\text{refl}}(x,z)$ for $z > 0$

It follows from the geometry that

$$V_{RR}(x,z) = 0, \quad \text{for } z > 0, x > 0$$

and

$$V_{RL}(x,z) = 0, \quad \text{for } z > 0, |x| < c. \tag{17}$$

For $z > 0$ and $x > c$, the diverging beam incident on the sample surface has passed through the spherical lens focus and has therefore suffered a phase shift of $-\pi$. However, there is no real Rayleigh wave focus on the sample surface in this case since the incident beam is diverging when it strikes the sample surface and the phase shift of $-\pi/2$ included in derivation of $V_R(x,z)$ no longer applies. Thus, for $z > 0$

$$V_{\text{refl}}(x,z) = \begin{cases} V_L(x,z) = V_R(x,z)\exp(-i\pi/2), & x > c, \\ 0, & x < c. \end{cases} \tag{18}$$

### E. The total voltage response $V(x,z)$

The total transducer voltage response function $V(x,z_0)$ is found by adding the specularly reflected, transmitted, and crack-scattered contributions as shown in expression (4). Typical $V(x,z_0)$ curves, calculated for a slot lens for defocus distance $z = -346$ and $-474\ \mu$m for crack displacement from the lens axis in the range $0 < x < 500\ \mu$m, are shown as solid lines in Fig. 13(a) and (b), respectively. The rapid fluctuation of $V(x,z)$ observed in Figs. 13 is due chiefly to the interference of the reflected surface wave contribution $V_{\text{refl}}(x,z)$ with the specular contribution $V_G(z)$. For small displacement $x$, the spatial period of the ripple is approximately one half of the period of the surface wave.

As mentioned earlier, it is assumed here that the surface wave reflection and transmission coefficients of the crack, $R$ and $T$, respectively, are constant for all angles of incidence. It is therefore necessary to use proper effective values for $R$ and $T$. Angel and Achenbach[12] have carried out an analysis

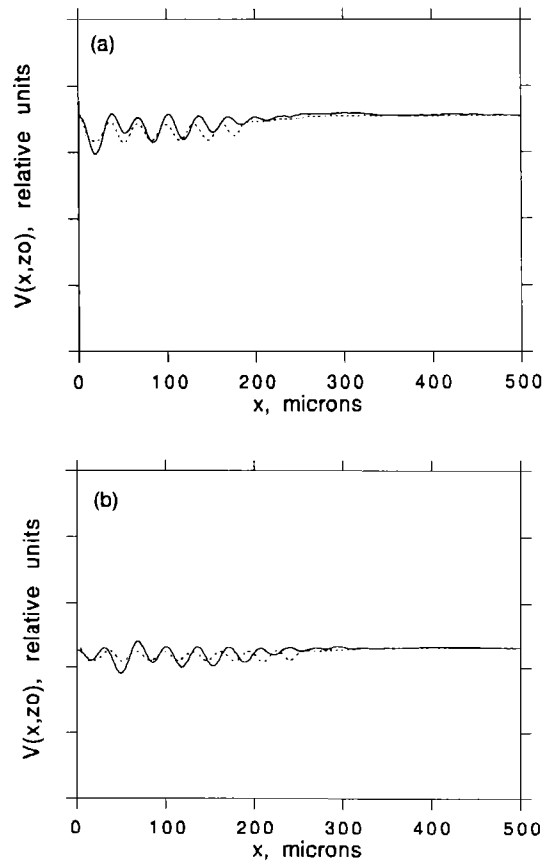


FIG. 13. Plot of $V(x,z_0)$ for a slot aperture lens; observed (solid) and calculated (dotted): (a) $z_0 = -346\ \mu$m and (b) $z_0 = -474\ \mu$m.

to find the scattering coefficients for various angles of incidence and crack depths and found the variation in $R$ and $T$ with angle of incidence to be only slight in the vicinity of normal incidence. The cracks observed in this work were very deep ($\approx 1$ mm), hence, the crack depth was assumed to be infinite when importing coefficient values from the reference.

When the slot is aligned perpendicular to the crack, the surface waves launched by the slot lens propagate in a narrow range of directions about the slot axis where the largest angle of incidence on the crack is given by $\sin^{-1}(w/\rho_R)$. For the lens used here, the above angle is 25°. The effective values for the slot lens were consequently chosen from the reference to be $R = 0.54$ and $T = 0$, which are reasonable values but strictly valid only at normal incidence.

## IV. EXPERIMENTAL MEASUREMENT OF $V(x,z_0)$

Measured $V(x,z_0)$ curves for the slot lens described earlier are displayed along with the above calculated curves in Fig. 13(a) and (b), over the range $0 < x < 500$ $\mu$m. The crack that was measured was produced in a glass microscope slide by first producing a small linear mechanical stress crack that was subsequently enlarged in length by application of thermal stress. Only samples with long straight cracks that appeared perpendicular to the sample surface were used in the measurements. It should be noted that the slot lens provides better agreement with theory in the neighborhood of the crack than does the circular lens as the ring focus formed under the condition $x = 0$ reduces to a pair of truncated circular arcs for a lens of narrow slot width which is more nearly consistent with the geometry assumed in the foregoing analysis. The remaining disagreement is thought to result from diffraction effects in the couplant.

### A. Extracting the surface wave reflection coefficient of a crack from the $V(x,z_0)$ data acquired using the slot lens

When the lens is negatively defocused and the crack lies at the lens axis, i.e., $x = 0$, $z < 0$, the scattered leaky rays trace paths that are the mirror images of leaky wave paths for the defect-free case. Refer to Fig. 14. Therefore, the microscope response at that point may be represented in terms of unperturbed contributions $V_G$ and $V_L$ as

$$V(x=0,z) = V_G(z) + TV_L(z) + R\left(\frac{V_L(z)}{2} + \frac{V_L(z)}{2}\right), \tag{19}$$

where the reflected contribution has been separated into two identical terms due to surface waves incident on the crack from the right and from the left. Note that if the discontinuity is not present, $T = 1$ and $R = 0$, and the expression reduces to the usual form $V(z) = V_G(z) + V_L(z)$. Under the condition $x \to 0$ and $z < 0$, $f_y$ tends to infinity and there is but one focus in the lens rod, located a distance $f_x$ above the aperture as shown in Fig. 7.

When the lens is moved from the crack in the positive $x$ direction as illustrated in Fig. 11, the surface waves incident from the left have to propagate an additional distance of $2x$ to the crack and back, thus gaining in phase by the factor $\exp(i2k_R x)$. Similarly, the rays incident from the right encounter the crack sooner and thereby lose the same value of phase. Neglecting other variations, which will be considered later, expression (19) can therefore be generalized for $x \neq 0$ as

$$\begin{aligned} V(x,z) &= V_G(z) + TV_L(z) \\ &\quad + R\frac{V_L(z)\exp(i2k_R x) + V_L(z)\exp(-i2k_R x)}{2} \\ &= V_G(z) + TV_L(z) + RV_L(z)\cos 2k_R x. \end{aligned} \tag{20}$$

Expression (20) can be used as a basis for the extraction of $R$ from $V(x,z_0)$ data but first the region of its validity should be determined. Since $f_y$ varies as $1/x$ for small $x$ in expression (14b), it rapidly approaches the plane of the transducer as $x$ increases from zero. A critical point is encountered where this focal point crosses the transducer plane, which occurs at $x = (f - R_0)\rho_R/2(D - f_x)$. For the lens used in this work, the location of the critical point is $x = 15$ $\mu$m. The amplitude of $V(x)$ calculated for $z = -346$ $\mu$m is plotted in Fig. 15 using an expanded $x$ scale. It can be observed from the graph that for $0 < x < 10$ $\mu$m the $V(x)$ varies approximately as a cosine function, in agreement with expression

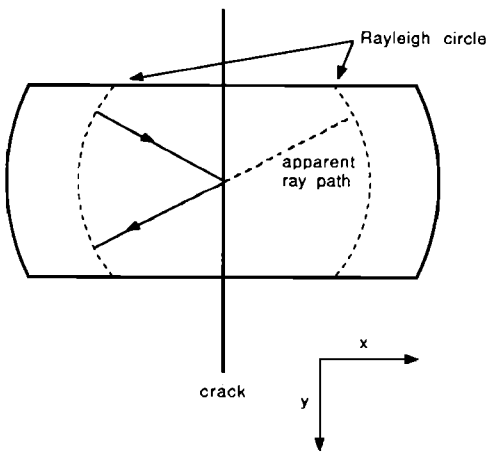


FIG. 14. Selected surface wave paths on the sample surface at $z < 0$ containing a crack parallel to the $y$ axis at $x = 0$.

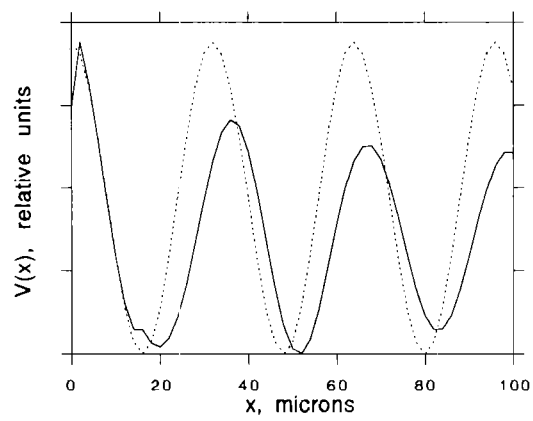


FIG. 15. Behavior in the vicinity of the crack: (a) calculated $V(x,z_0 = -346\mu\text{m})$ for the slot aperture lens (solid) and (b) the function $\cos(2k_R x)$ (dashed).

(20). As discussed above, the model for $V(x)$ fails at $x = 0$. At that point, however, the microscope response is reasonably well described by (19). Thus, expression (20) will be assumed to be valid for small $x$ and be used for extracting a value for $R$.

The acoustic microscope employed in this work measures only the amplitude of the transducer voltage $|V(x,z)|$. Taking the square of the amplitude of (20) gives

$$|V(x,z)|^2 = |V_G + TV_L|^2 + 2|V_G + TV_L||V_L R| \times \cos[2k_R x + \phi(z)] + |V_L R|^2 \cos^2 2k_R x, \tag{21}$$

where $\phi(z) = \arg[V_G(z)] - \arg[V_L(z)] - \arg(R)$. Since the measurement is carried out on a system where the smallest translational step in $x$ is 2 $\mu$m, there is a positional uncertainty of less than 1 $\mu$m in locating the true $x = 0$ point. The resultant error in $x$ can be included as a constant phase term in $\phi$ in (21).

When the $V(x,z_0)$ measurement is performed at $z_0$ corresponding to a maximum or minimum in voltage, $V_G$ and $V_L$ are either exactly in phase or of opposite phase, or, respectively, $V(z) = |V_G| \pm |V_L|$ and the magnitude of $|V_L|$ can be determined by subtracting $|V_G|$ from $V(z)$. To find $|V_G|$, the $V(z)$ of a Teflon sample is scaled to match the $V(z)$ of the homogeneous sample material at large $|z|$, where $|V_L| \ll |V_G|$.

Evaluating the $|V_L|$ and $|V_G|$ at several local $V(z)$ maxima and minima gives $|V_G| > 10|V_L|$ in which case the last the term in (21) is small compared to the other terms and can be neglected. To remove the $x$-independent term $|V_G + TV_L|^2$ from (21), $|V(0,z)|^2 - |V(x,z)|^2$ is evaluated as

$$\begin{aligned} &|V(0,z)|^2 - |V(x,z)|^2 \\ &\quad = 2|(V_G + TV_L)V_L R|\cos\phi(1 - \cos 2k_R x) \\ &\qquad - 2|(V_G + TV_L)V_L R|\sin\phi \sin 2k_R x. \end{aligned} \tag{22}$$

The objective here is to find the coefficients multiplying the $(1 - \cos 2k_R x)$ and $\sin 2k_R x$ terms. When (22) is evaluated at two points, say, $x_1$ and $x_2$, a system of two equations containing the two undetermined coefficients $A$ and $B$ may be written as

$$\begin{aligned} &A(1 - \cos 2k_R x_1) - B \sin 2k_R x_1 \\ &\quad = |V(0,z)|^2 - |V(x_1,z)|^2, \\ &\text{and} \\ &A(1 - \cos 2k_R x_2) - B \sin 2k_R x_2 \\ &\quad = |V(0,z)|^2 - |V(x_2,z)|^2, \end{aligned} \tag{23}$$

where $A$ and $B$ are independent of $x$ and given by

$$\begin{aligned} A &= 2|(V_G + TV_L)V_L R|\cos\phi \\ &\text{and} \\ B &= 2|(V_G + TV_L)V_L R|\sin\phi. \end{aligned} \tag{24}$$

The system (23) can be solved for $A$ and $B$ from the measured data. From (24) it follows that

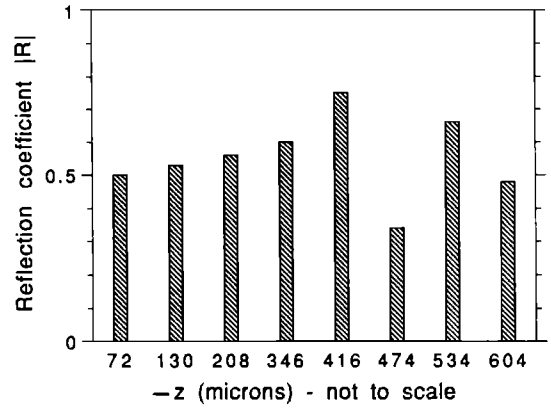


FIG. 16. Magnitude of surface wave reflection coefficient deduced from measurements made of a cracked glass sample using the slot lens.

$$\begin{aligned} &\sqrt{A^2 + B^2} = 2|(V_G + TV_L)V_L R| \\ &\text{and} \\ &\phi = \tan^{-1} B/A. \end{aligned} \tag{25}$$

The factor $|(V_G + TV_L)|$ in (24) is found by noting that it is exactly the square root of the $x$-independent term in (21) and can therefore be obtained by substituting (24) and (25) into (21) for any small $x$. Finally, $|R|$ is found from (25) using the value of $|V_L|$ deduced from the unperturbed $V(z)$'s of glass and Teflon, in the procedure described above.

Since the system of equations (23) requires the knowledge of $V(x,z)$ at only two $x$ locations in addition to the value $V(0,z)$, it is possible to use the $V(x,z)$ data at other points to create additional (redundant) equations and simultaneously solve any two of them. The resulting values of $|R|$ can then be checked for consistency and if in reasonable agreement can then be averaged.

The results of applying the above algorithm to extract $|R|$ from $V(x)$ measured at different defocus distances $z$ are presented in Fig. 16. Since the signal detected by the transducer weakens significantly as $|z|$ increases, only $V(x,z)$ measured at smaller values of $|z|$ appear to be reliable as they are the least corrupted by noise. It is seen that the values of $|R|$ in Fig. 16 for $z > -210\,\mu$m compare favorably with the value $|R| = 0.54$ deduced by Angel and Achenbach[12] for a deep crack. Furthermore, the average value of $|R|$, calculated for all $z$ in Fig. 16, is found to be 0.55.

Angel and Achenbach[12] have also conducted a study of the dependence of $|R|$ on the depth of a crack, which conceivably could be used to gauge crack depth from $V(x,z)$ measurements made with the slot lens by the technique described above.

## V. CONCLUSIONS

A ray theoretic approach that accounts for diffraction effects in the lens rod was used to predict the $V(z)$ behavior of the slot lens for the cases of materials that do not possess leaky surface modes as well as those that do. The dynamic range in $V(z)$ appears to differ somewhat between theory and experiment, as matching values at focus results in a somewhat smaller observed $V(z)$ at large negative defocus distances, which may be due to the neglect of diffraction in

the couplant. Neglect of this diffraction is more worrisome than in the case of the circular point-focus lens that was treated by this method earlier. In spite of this, the results are far superior to the original ray method and are computationally simpler than the angular spectrum approach of Atalar.[13]

The utility of the slot lens is demonstrated by measuring the angular dispersion of surface wave velocity for a $y$-cut quartz sample. The largest velocity error was observed to be about 1%. The image scanning capability of the lens had been previously documented in the cited references.

The fact that the lens has application in crack studies is shown by theory and observation. An algorithm is worked out that permits a determination of the reflection coefficient of the crack to a leaky surface wave. This makes possible, at least in principle, a determination of crack depth from $V(x,z_0)$ measurements. The fact that the slot lens has image scanning potential as well as being more tolerant to small angular misalignment when compared with the line focus lens indicates that it may have use in obtaining images of cracked surfaces.

## ACKNOWLEDGMENT

The work of D. Chizhik was supported by a research fellowship from AFOSR, Bolling AFB.

[1] D. A. Davids, P. Y. Wu, and D. Chizhik, "Restricted aperture acoustic microscope lens for Rayleigh wave imaging," Appl. Phys. Lett. **54**, 1639–1641 (1989).

[2] D. A. Davids and H. L. Bertoni, "Bow-tie transducers for measurement of anisotropic materials in acoustic microscopy," Proc. IEEE Ultrasonic Symp. **2**, 735–740 (1986).

[3] D. A. Davids, D. Chizhik, and H. L. Bertoni, "Measured characteristics of an acoustic microscope having a bow-tie transducer," Proc. IEEE Ultrasonic Symp., 763–766 (1988).

[4] H. L. Bertoni, "Ray-optical evaluation of $V(z)$ in reflection acoustic microscope," IEEE Trans. Sonics Ultrason. **SU-31**, 105–116 (1984).

[5] D. Chizhik, D. A. Davids, and H. L. Bertoni, "A diffraction corrected ray theory for the acoustic microscope," Proc IEEE Ultrasonic Symp., 731–735 (1991).

[6] M. G. Somekh, H. L. Bertoni, G. A. D. Briggs, and N. J. Burton, "A two-dimensional theory of surface discontinuities with the scanning acoustic microscope," Proc. R. Soc. London Ser. A **401**, 29–51 (1985).

[7] D. A. Rebinsky and J. G. Harris, "An asymptotic calculation of the acoustic signature of a cracked surface for the line focus scanning acoustic microscope," Proc. R. Soc. London Ser. A **436**, 251–265 (1992).

[8] J. N. Tjotta and S. Tjotta, "An analytical model for the nearfield of a baffled piston transducer," J. Acoust. Soc. Am. **68**, 334–339 (1980).

[9] G. A. D. Briggs, J. M. Rowe, A. M. Sinton, and D. S. Spencer, "Quantitative methods in acoustic microscopy," Proc. IEEE Ultrason. Symp., 743–749 (1988).

[10] J. Kushibiki and N. Chubachi, "Material characterization by line-focus-beam acoustic microscope," IEEE Trans. Sonics Ultrason. **SU-32**, 189–212 (1985).

[11] D. Chizhik, D. A. Davids, H. L. Bertoni, and M. G, Somekh, "A modified ray theory for predicting the $V(x,z)$ response of a point focus acoustic microscope in the presence of a crack," J. Acoust. Soc. Am. **91**, 3285–3290 (1992).

[12] Y. C. Angel and J. D. Achenbach, "Reflection and transmission of obliquely incident Rayleigh waves by a surface breaking crack," J. Acoust. Soc. Am. **75**, 313–319 (1984).

[13] A. Atalar, "An angular spectrum approach to contrast in reflection acoustic microscopy," J. Appl. Phys. **49**, 5130–5139 (1978).